# Mapping Chicago Area Urban Tree Canopy Using Color Infrared Imagery

**Jeanette McBride**

A Master thesis presented to

Department of Physical Geography and Ecosystem Analysis

Centre for Geographical Information Systems

of



by

**Jeanette McBride**

in partial fulfilment of the requirements

for the degree of Master in Geographical Information Science

Supervisor:

Ulf Helldén
Department of Earth and Ecosystem Sciences
Lund University

i

# ABSTRACT

Satellite imagery has been used to produce highly-accurate land cover maps, even effectively discriminating between vegetation types. While land cover classification based on differences in pixel values in one or more spectral bands is an effective way of mapping large areas, the coarse resolution of freely available satellite images is not suitable for mapping urban environments. In Illinois, USA, color infrared (CIR) aerial photos with a resolution of two meters are freely available via download. This study explores the possibility of developing a template for mapping tree canopy in an urban environment using two-meter resolution CIR imagery.

The possibility of applying the same set of classification criteria to various images from the greater Chicago area, rather than evaluating and determining classification values for each image, was tested. The ultimate goal is to provide less-advanced GIS users with a simple procedure for generating a tree canopy map using the above-described imagery. Due to differences in image capture conditions that can result in dissimilar spectral characteristics across images, it is expected that such a generalized approach would compromise classification accuracy. The limits to this type of general template for mapping urban tree canopy, and the classification method that is most effective when applied to several different images, form the focus of this paper. One image was used for model development, and the most successful model was applied to three adjacent images for further evaluation.

Nine vegetation indices as well as the three spectral bands were tested for potential to discriminate between woody vegetation and grass in a land cover classification. An NDVI layer was created, and those pixels with NDVI below a minimum value were excluded from further evaluation, leaving a raster layer representing only green biomass. General statistics for pixel values in polygons identified as grass or canopy were then evaluated to determine the best ranges for assigning vegetation pixels to either the tree canopy or grass class. A simple raster calculator method was used to create land cover maps using the range of values returned by general statistics for the two vegetation types in each vegetation index or spectral band. Three automated computer classification methods were also tested for comparison against these results.

Results from the classification of the first image found both the red and green spectral

band values capable of producing a land cover classification with 82% accuracy. The automated classifications ranged from 79 to 80% in overall accuracy. Two indices, NIR/green and (NIR+red+green/3), also resulted in 80% overall accuracy. Although none of the indices, spectral bands or automated classifications resulted in a land cover classification of greater than 81% accuracy, when the model developed on the first image was extended to three adjacent images, both the red and green spectral band values, and two of the vegetation indices, produced land cover classifications with greater than 76% overall accuracy. The model that produced the best tree canopy classification results when applied to all four images defined tree canopy pixels as those where NDVI > 0.119 and (NIR+red+green)/3 <=132. This classification resulted in an overall accuracy of 81% for the expanded study area with a producer's accuracy for the final canopy raster layer of 88.5%. User's accuracy was 70.4%, the kappa coefficient was 0.705, and the kappa for the canopy class was 0.547. Aeral difference was +25.7%.

For a quick canopy raster layer that will probably result in 80% overall accuracy, and producer's accuracy for canopy class approaching 90%, the (NIR+red+green)/3 index is the best solution when using Chicago area NAIP imagery captured during mid-summer.

**Keywords**: tree canopy, color-infrared imagery, urban forest, vegetation indices, NDVI, remote sensing, Chicago

# Contents

## 1. Introduction and objectives

### 1.1  Interest in urban canopy quantification

Even in Illinois, nicknamed "the prairie state", people are becoming increasingly aware of the benefits provided by trees.  Not only do they produce oxygen for us to breathe, trees also remove particulate matter and other pollutants from our air.  Shade from trees can provide evaporative cooling in summer and block winter winds, reducing energy use in buildings.  Additionally, urban trees have a positive effect on environmental quality, and help regulate storm water run-off (Nowak *et al* 2010).  And on a purely aesthetic level, trees beautify our landscape and promote a sense of pride in our communities.

The city of Chicago has devoted significant time and money to measuring the extent of its tree canopy (Kowal 2007).  Many other municipalities in the Chicago area are looking for a way to measure the amount of tree canopy cover within their borders.  Sometimes the intent is to establish a tree canopy baseline to be maintained when new construction is proposed, other times a town may be trying to determine which of its neighborhoods are lacking in trees, and in some cases even the possibility of carbon sequestration generates an interest in quantifying tree cover. While municipal forestry departments usually have some kind of tree inventory, simple numbers of trees do not provide adequate information for calculating the area of tree canopy.

Fortunately, the use of GIS (geographic information systems) and remotely-sensed imagery provides a reliable way of estimating canopy cover.  Using computer technology, it is possible to quickly generate land cover maps based on remotely-sensed data.  Although this type of land cover classification is never perfect, its accuracy is usually acceptable, and a map layer can be completed quickly.  Remotely-sensed imagery can also provide a means for monitoring canopy cover changes and even tree health through comparison of images over time.

### 1.2  Satellite imagery versus color-infrared aerial imagery

Freely available satellite imagery commonly contains up to seven different spectral bands,  including several not visible to the human eye.  These extra bands often contain important differences in spectral values that enable the computer to accurately sort the pixels into land use classes.  Multi-spectral data from Landsat and other satellites have been found suitable for discriminating vegetation from non-vegetated land cover, but the coarse resolution of this imagery (usually 30m) is not appropriate for mapping heterogeneous urban environments.

1

Although tree canopy GIS datasets exist for the seven-county Chicago region, these are based on 30m satellite imagery. Individual tree crowns, and even yards adjacent to houses, are too small to be discriminated at this spatial resolution. Therefore, these datasets do not provide a realistic representation of the actual tree cover in the region. While high resolution satellite imagery has been used by the city of Chicago for urban forest mapping (http://www.rfpmappingllc.com/chicagoutc), this imagery is not freely available, and therefore not accessible to most municipalities.

An alternative remotely-sensed data type is the color infrared (CIR) aerial image. While a regular three-color image is comprised of the bands red, green and blue, CIR film is comprised of bands in the near infrared (NIR), red and green wavelengths. NIR wavelengths, which are not visible to the human eye, are slightly longer than red wavelengths. Blue wavelengths, a part of natural color film, are filtered out of CIR images. CIR film has been used for many applications involving vegetation, the primary purpose being to monitor the health of crops or forests. Using spectral signatures, which refer to the way a particular object reflects and absorbs light at different wavelengths, it is even possible to distinguish different plant species from their tone in an image (Fig. 1).
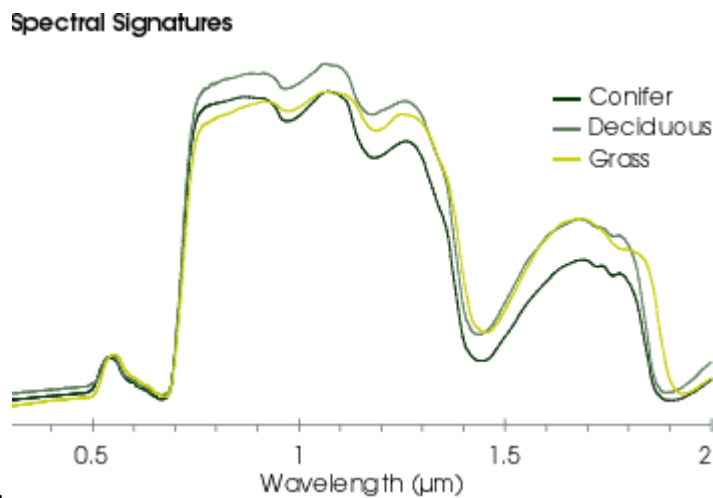


Figure 1. NASA Earth Observatory

Conventionally, CIR images display the NIR band data as red, the red band as green, and green wavelengths appear blue. Because healthy green vegetation appears as bright red, a CIR image is also known as a "false color" image. Variations in the red color can indicate vegetation

that is stressed due to insect infestation, soil deficiencies, and over or under watering. So while CIR imagery does not have as many spectral bands as satellite imagery, the NIR band makes it useful for vegetation studies. CIR digital orthophoto quarter quadrangles (DOQQs) for the Chicago area are available for free download through The Illinois Natural Resources Geospatial Data Clearinghouse. Using this high resolution imagery, it should be possible to extract pixels representing street trees in the urban landscape.

### 1.3  Objective

The aim of this study is to determine the feasibility of creating a raster layer representing the Chicago area tree canopy using two-meter resolution CIR imagery. The intended results would be of a high enough quality to be useful to local government, both at the town and county or regional level, in areas where most tree cover is in the form of "street trees" or urban plantings. This study will determine the most effective basic method of creating a tree canopy raster that would be helpful for municipal land managers working to develop long-term management plans for sustaining healthy urban tree populations. The methods evaluated in this study and the resulting canopy map might help people in the Chicago area and beyond develop a better understanding of the extent of their urban forest.

In a preliminary investigation using CIR imagery from the Chicago region, it was possible to separate green vegetation from built-up areas using the normalized difference vegetation index (NDVI), but when attempts to separate tree canopy from grass resulted in a great deal of overlap in NDVI values. This study will explore the effectiveness of other vegetation indices for this task. When the method for attaining the most accurate tree canopy classification has been identified, the results will be used to create a raster representing the tree canopy for one USGS quadrangle (approximately 142.45 square kilometers). The intention is to produce a GIS layer that can be used to calculate the extent or percentage of tree canopy in different parts of the study area. Although some pixels will be classified incorrectly – some areas of lawn that are erroneously included in the tree canopy map and some fragments of tree canopy that are classified as grass – an estimation of accuracy will be included to give users an understanding of the possible applications for this raster.

Although true-color imagery could also be evaluated for this type of urban vegetation discrimination, currently available cost-free high-resolution true-color imagery for the region

3

was captured during leaf-off period between March 28 and May 4, 2005.  The late winter/early spring timing of this imagery renders it irrelevant for canopy mapping.

Though somewhat technical, the results of this study and the explanation of the methods should be accessible to most GIS users.  Many GIS users may not know about NDVI or other methods for creating land use maps from CIR imagery.  Hopefully it will provide a relatively simple example of how to create an acceptably accurate urban tree canopy map using readily available materials.

## 2.  Background
### 2.1  Vegetation indices

In some remote-sensing land cover classifications, the pixel values from single spectral bands are tested for correlation against other data.  More often, pixel values from multiple bands of imagery are combined using indices to enhance the reflectance contrast between different wavelengths.   Ratio indices make use of differences in reflectivity by combining wavelengths that have the opposite effect in a given cover type: one increases while the other decreases.

Tucker (1979) used ground-collected insitu spectrometer data to test the correlation between vegetation and spectral bands and concluded that infrared/red and related infrared and red linear combinations were superior to green/red and related green-red linear combinations for the purpose of monitoring vegetation.

Jackson and Huege (1991) explain how vegetation indices have been developed to extract pixels representing plants.  This is an improvement over simple reflectance values because solar irradiance varies with time and atmospheric conditions, meaning that the same surface will not necessarily have the same reflectance at any given time.  Hence, combining data from two or more spectral bands using a vegetation index makes it possible to enhance the visibility of vegetation while minimizing the extraneous effects of atmosphere and soil background.  Vegetation indices derived from satellite imagery have been widely used to create land cover maps, monitor vegetation conditions, map land cover change, and even to distinguish between healthy and unhealthy stands of trees.

Jordan (1969) developed the ratio vegetation index (RVI = NIR/red) as a way of using remote-sensing to measure leaf area per area of ground.  Differences between pixel values in the red and NIR bands is a strong indicator of the amount of photo-synthetically active green

biomass. In dense green vegetation, there is little red reflectance but much NIR reflectance, so a large difference in pixel values between these two bands indicates the presence of healthy plant life. According to Jordan, the greater the leaf area, the greater the difference between red and infrared radiation.

Although RVI is sensitive to heavy vegetation cover, it does not perform well in sparse vegetation. It was this drawback that led to the development of the normalized difference vegetation index (NDVI). NDVI was developed by researchers at the Remote Sensing Center of Texas A & M University and at NASA's Goddard Space Flight Center in the early 1970's using data from the multispectral scanner on LandSat-1 (Rouse *et al* 1973 ). As with the RVI, because vegetation has high reflectance in the NIR band and low reflectance in the red band, the ratio expressed by the NDVI formula (NIR-R)/(NIR+R) highlights green biomass, or the presence of chlorophyll. NDVI returns values ranging from -1 to 1, with values for green vegetation generally falling between 0.2 and 0.8. Although NDVI is only one of several indices mentioned in literature about plant health, it has become the most commonly used vegetation index.

NDVI is less sensitive in areas of dense vegetation, where the correlation between NDVI and abundance of vegetation breaks down. Researchers have continued to develop other vegetation indices, usually using multispectral satellite imagery. A variation on NDVI developed by Deering *et al* (1975), the transformed vegetation index (TVI) uses the square root of NDVI + 0.5, with the 0.5 added to keep pixel values positive. Xu, Gong and Pu (2003) modified NDVI by raising pixel values from the red and NIR bands to the second power (NIR^2-red^2/NIR^2+red^2), and again in another modification that raises values to the third power.

The chlorophyll index (the ratio between the green band and red band, or green/red) is expected to perform better than NDVI in urban areas where biomass is contrasted against a usually light background with high reflectance in both the red and NIR bands (Nichol and Lee, 2005).

To address NDVI's sensitivity to the properties of soil background, which can be significant in sparse vegetation, the soil-adjusted vegetation index (SAVI) was developed. This index uses the NIR and red band along with a soil brightness correction factor to minimize the spectral variance introduced by background soil type (Huete 1988).

The GNDVI ((NIR-green)/(NIR+green)) uses the green spectral region instead of red to enhance the presence of chlorophyll. Gitelson, Kaufman and Merzlyak (1996) developed this

vegetation index based on the conviction the information from the green spectral band should not be so easily dismissed, being that green provides our visual clue to vegetation, and might be more effective in a vegetation index than NIR.

Linear vegetation indices such as the difference vegetation index (DVI=NIR-red) developed by Clevers (1988) don't compensate for different atmospheric conditions, which is one reason ratio indices are preferable to linear ones.

## 2.2 Land cover classification in urban areas

Literature on remote sensing applications in urban environments is limited in comparison to natural resource monitoring. Generating accurate land cover maps using remotely-sensed imagery in urban settings is a known problem due to the complex spatial arrangement of small patches of a variety of land cover types. NDVI, when obtained using medium to coarse resolution multispectral satellite data may introduce large errors into landscape classifications with high spatial heterogeneity such as urban areas. Buyantuyev, Wu and Gries (2007) conducted an accuracy assessment using NDVI values derived from coarse resolution satellite data and concluded that spectral mixture analysis (a process for addressing the problem of 'mixed pixels', or those pixels encompassing more than one land cover) is necessary when using this type of data in urban landscapes. Lu and Weng (2004) used Enhanced Thematic Mapper Plus (ETM+) satellite data with 30 meter spatial resolution to map ten different land use classes in Indianapolis, IN. Since many land cover types occur as heterogeneous mixtures in the urban context, even when viewed at spatial scales as fine as 2m by 2m, they also recommend using spectral mixture analysis for improving classification accuracy.

In addition to mixed pixels, shadows can further complicate the classification of urban imagery. Zhou *et al* (2009) addressed the fact that a significant proportion of high spatial resolution imagery in urban areas can be affected by shadows. The authors used a combination of CIR imagery and LIDAR to test three methods for land cover classification of shaded areas in Baltimore Co., MD. Results indicate a considerable proportion of shaded pavement was misclassified as shaded grass. They determined the best method for correcting shadow effects in urban areas is by replacing shaded pixel values using image data collected at a different time.

### 2.3 Trees and NIR spectral data

Researchers studying urban areas have used NDVI to create maps of vegetation within cities and towns, yet the task of separating common urban vegetation types (particularly trees and grass) using NDVI has been problematic.  Successful separation of grass from tree canopy usually requires date-specific imagery that capitalizes on dormant or dry-season spectral differences.  Price, Guo and Stiles (2002) working in eastern Kansas found it crucial to use imagery from a particular month.

Peña-Barragán *et al*. (2004) used both conventional color and CIR imagery to try and separate legumes and grasses from tree canopy and bare ground in olive groves in Spain.  Using four color bands (blue, green, red and NIR), the authors computed 22 indices, and also evaluated each spectral band for its ability to discriminate between the land cover types.  The summer conventional color images and three vegetation indices that use data from the blue spectral band enabled them to discriminate cover crops from other land use with an average accuracy of 85%. Two of these indices discriminated olive trees from other land uses with an average accuracy of 92%.  Vegetation indices using the red band produced the best results for discriminating olive trees from other land cover.  The authors concluded that conventional color photographs worked better than CIR, partly because vegetation indices that use the blue band were best for cover crop discrimination.

Xu, Gong and Pu (2003) used Landsat Thematic Mapper (LTM) imagery captured in August to estimate crown closure in oak savannas in California.  In addition to assessing correlation between crown closure and individual image bands, the authors tested NDVI and their own variation on this index, which they call NDVIN.  (NDVIN raises NIR and red values to the second or third power before applying the NDVI formula.)  Because grasses are brown in California in August, the reflectance of dry grasses is higher than oak leaves in the visible bands. The authors found that the red band had the highest correlation with crown closure (a negative correlation), while the NIR band had a low positive correlation.  The RVI offered no improvement over the correlation achieved by the red band itself, because of the poor correlation between NIR and crown closure.  NDVI, however, resulted in a slight improvement due to the variability of the NIR band among land cover types and a generally stable red band.  The authors experimented with modifying NDVI to $(NIR^2\text{-}red^2/NIR^2\text{+}red^2)$**,** and again for the third

power. They found that using the second and third powers resulted in better regression results, but that the fourth power and higher were not helpful.

Carreiras, Pereira and Pereira (2006) wanted to estimate tree canopy cover in a savanna landscape of southern Portugal using vegetation indices based on Landsat images captured in late summer. They used multiple regression to model the relationship between tree canopy cover evident in aerial photos and reflectance values from the satellite imagery. The best regression fit was with individual values from two red and two NIR channels, and NDVI was almost as reliable. The late summer origin of the imagery was crucial, as the understory in these savannas is a light color at that time of year (dry vegetation and soil). The authors stress the benefit of using imagery from a date when there is maximum spectral contrast between the tree canopy and understory.

Nichol and Lee (2005) used multispectral IKONOS and CIR images to test the effectiveness of NDVI and the chlorophyll index for estimating both vegetation cover and vegetation density in Hong Kong. Pre-shadow removal results showed the IKONOS red band to be the best indicator of vegetation cover. The best CIR pre-shadow removal results were using the chlorophyll index to measure vegetation density and using the red band to detect vegetation cover. The authors explain that vegetation density estimates were slightly more accurate than vegetation cover estimates because as vegetation density increases, the green/red ratio increases and improves the distinction between grass and trees. The authors preferred the chlorophyll index to NDVI for this study because the imagery was collected during the dry season when the NIR band has reduced reflectance in vegetation. Hence reflectance of vegetation in the NIR band was no higher than in built-up areas, but was lower than built-up areas in both the green and red bands. Their results found that while NDVI could be used to distinguish between vegetation and built-up areas, it could not separate grassy vegetation from tree cover.

Ward, Phinn and Murray (2000) examined urban growth between 1988-1995 southeast of Queensland, Australia using LTM data bands 1-5 (blue, green, red, NIR, middle infrared) and 7 (middle infrared). The woody component of this vegetation is made up mostly of eucalyptus, which has distinctly different spectral values from crops and grassland. Neither NDVI nor SAVI provided consistent results within the urban areas examined. The images they were working with were captured in June, which is a dry time, so the non-woody vegetation had dried up, exposing areas of soil. The authors conclude that land cover composition in urban areas can be

successfully classified if the images are carefully processed – in their case, beginning with an unsupervised classification.

Kowal (2007) set out to precisely measure the spatial extent of tree canopy in the city of Chicago in order to quantify its financial worth. He used merged one-meter panchromatic (black and white) and 4-meter multispectral (red, green, blue, and NIR) IKONOS-2 imagery to create a 1-meter resolution merged four-band multispectral dataset for the entire 606 square kilometer area of the city of Chicago. Kowal states that, in general, vegetated land will return NDVI values ranging from 0.19 to 0.9, with higher ranges corresponding to higher density of vegetation. NDVI values of less than 0.3 did not correspond to any tree canopy areas within his 1-meter resolution merged dataset. While some of the pixels could be clearly identified as tree canopy or not, most could not be. Areas that could be decisively declared were set aside, then another round of unsupervised classification was conducted on the remaining portion of the data. Eventually all cells believed to depict tree canopy were assigned value of one, all others a value of zero.

Less than 1% of Kowal's data was found to contain problem areas. One of these problems consisted of small areas of very lush (probably fertilized) grass that were classed as trees due to similarities in the spectral signatures to those of certain tree crowns. These showed up as scattered individual pixels classified as tree canopy but clearly within areas of non-tree vegetation. Another type of problem was small portions of tree crowns being classed as grass. In order to improve upon this 99% accuracy, Kowal developed a model to filter out isolated individual scattered cells classed as canopy and another model to identify small groups of one to three cells classed as non-tree but surrounded by tree. In this way he was able to re-classify isolated cells that almost certainly belonged to the same vegetation type as the surrounding pixels.

### 3. Methods

### 3.1 Study area

The Chicago metropolitan area, which refers to a seven county area including the city of Chicago and its surrounding suburbs, is located in northeastern Illinois, U.S.A., bounded by the Wisconsin state line on the north and Lake Michigan on the east (Fig. 2). Latitude ranges from 41˚15' to 42˚30', and longitude from -88˚37'30" to -87˚30'. Topography is relentlessly flat, with

total elevation in the area ranging from 128.2 meters along the Kankakee River in northern Will County to 360.7 meters on the Fox Lake Moraine in the northwestern part of the area.  The climate is continental, and while not quite as harsh as North American plains, is characterized by cold winters and hot, humid summers. Temperatures range from -18C to 38C and the number of days between killing frosts ranges from 122 to 152.  Annual average precipitation is 840mm, with about 67% occurring during the growing season, with great variation due to periodic summer drought.

The imagery evaluated in this study is located in the central part of this region with its boundary defined by the USGS Hinsdale 7.5' quadrangle(quad)  map.  The area within the Hinsdale quad  includes 11 towns in both eastern DuPage and western Cook counties where population ranges from 411.7 to 2402 per square kilometer.  Per capita income likewise varies widely in this area, from $39,795 to $76,688.  The eastern most towns, located in Cook County, generally have a higher population density and lower per capita income, and are therefore more similar in character to Chicago than to the more affluent suburbs further west.  The more affluent towns are characterized by larger yards, fewer industrial sites, and more open space.



Figure 2.  Location of the Chicago metropolitan area in northeastern Illinois, U.S.A.

The population in the towns contained within the Hinsdale quadrangle was 160,415 at the time of the 2000 census.  The landscape is characterized by high and medium density urban built-up areas, with most former agricultural areas having been developed before the 1970's.  The landscape includes eight forest preserve properties with a total area of approximately 12 square kilometers, including the Salt Creek Greenway, which runs along Salt Creek and the Des Plaines River, both of which are generally wooded.

When European settlers first arrived in this area, vegetation was approximately 70% prairie, with blocks of timber generally restricted to locations along watercourses or other fire-protected sites (Davis 1977).  The dominant species were the somewhat fire-tolerant white and bur oak.  Estimates of historic tree density suggest open canopy conditions were quite common in areas of timber, with forest-type tree densities restricted to fire-protected sites (Bowles and McBride, 2002).  European settlers began widespread farming in the mid 1800's, and to protect their property and towns, they suppressed the prairie wildfires, thereby eliminating one of the main forces that shaped the natural vegetation of the Chicago region.

It is unlikely that many of the trees left in our urban and suburban tree canopy date from the days before European settlement.  Trees that weren't harvested for building material were usually removed for road or other construction, or mortally damaged during construction projects around them.   Instead, the Chicago urban forest contains a varied mix of native species that existed prior to European settlement and exotics introduced more recently.  The city and many of its suburbs have a forester on staff and maintain a budget dedicated to the planting and care of thousands of parkway (or "street") trees.  A 1987 estimate placed tree cover within the city boundaries at 11% (Nowak *et al* 1996).

Especially in the suburbs, but in some of Chicago's green spaces as well, Kentucky bluegrass, or "lawn", is highly valued as a landscaping theme.  While slightly less popular than they used to be (due to the increasing popularity of native landscaping alternatives that are better adapted to the climate), lawns are still a big business.  There is an entire lawn-care industry built around regular chemical applications of fertilizers intended to keep this alien grass a healthy monoculture during the stressful heat of summer.  With neighborhood pressure to keep a perfect lawn, it is not unusual for homeowners to water their grass during dry periods.  The fact that the perfect lawn is somewhat of  a status symbol means that even in summer there are innumerable patches of grass in various shades of green visible in aerial photos.

### 3.2  Image data acquisition

The specific imagery for this study is the 2004 Illinois National Agriculture Imagery Program (NAIP) Digital Orthophotography Quarter Quadrangle (DOQQ) data.  NAIP acquires color-infrared digital ortho imagery with a two-meter resolution during the agricultural growing seasons in the continental U.S.  This imagery has been created for 102 Illinois counties in the Universal Transverse Mercator (UTM) coordinate system with a NAD83 datum.   The pixel row count for each image is 3798 and the column count 2936.  The images are characterized by 24-bit pixels with waveband reflectance values ranging from 0 to 255 characterizing each pixel in each of the three bands (NIR, red and green).  NAIP imagery can contain as much as 10% cloud cover per tile.  The tiling format of NAIP imagery is based on a 3.75' x 3.75' quarter quadrangle, with the extent covered by each quarter quadrangle being approximately 45 square kilometers.

These DOQQs are available for free download in Mr. Sid format from the Illinois Natural Resources Geospatial Data Clearinghouse, an affiliate of the National Spatial Data Infrastructure Clearinghouse Network.  Hosted by the Illinois State Geological Survey since July 1, 1997, the Illinois Clearinghouse provides GIS data to diverse set of organizations including government agencies, teachers and students, and private sector businesses. People who enjoy exploring the outdoors also frequent the Illinois Clearinghouse to download various GIS layers.

The specific DOQQs evaluated in the project were captured in July 2004. Both average temperature and total precipitation for the Chicago area were slightly above normal that summer. The DOQQs used for the testing and model development portion of this study are contained by the USGS Hinsdale 7.5' quadrangle map, which is located in the central western part of the study area (Fig. 3).  The DOQQ of the northwest quarter of the quadrangle (Hinsdale NW) was chosen for model development because it includes a mix of urban land cover types that are representative of both the higher-density and lower-density towns in the Chicago area.  Hinsdale NW and Hinsdale SW were flown on July 28, 2004, while Hinsdale NE and Hinsdale SE were flown on July 11.   At this point in the summer, trees would be fully leafed-out and at least two months away from senescence.  Meticulously cared for lawns, especially those on golf courses, would be lush green, while less pampered grass would be more green than yellow, given the higher than average rainfall.
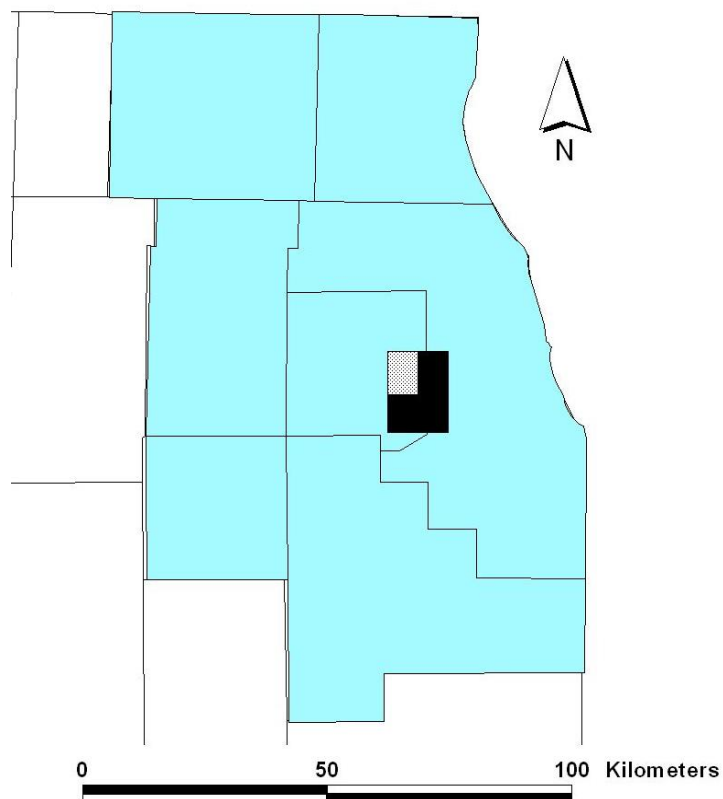
Figure 3.  Location of the Hinsdale USGS quadrangle within the seven county Chicago region and  Hinsdale NW DOQQ overlay.


After download, the images were decompressed and converted to .TIF format.  Statistics for pixel values in each of the spectral bands in each DOQQ were derived and recorded for further reference (Table 1).  Histograms of each spectral band in each image were also evaluated to assess the similarity of image characteristics (appendix A, B, and C).

Table 1. General statistics for each spectral band in the four Hinsdale DOQQs.

|  | DOQQ | Minimum value | Maximum value | Mean | Standard Deviation |
|---|---|---|---|---|---|
| NIR | HinsdaleNW | 41 | 255 | 135.60 | 32.73 |
|  | HinsdaleNE | 14 | 255 | 148.21 | 48.17 |
|  | HinsdaleSW | 31 | 255 | 147.15 | 34.39 |
|  | HinsdaleSE | 26 | 255 | 152.90 | 45.94 |
| Red | HinsdaleNW | 32 | 255 | 110.16 | 31.49 |
|  | HinsdaleNE | 3 | 255 | 105.87 | 47.21 |
|  | HinsdaleSW | 36 | 255 | 121.54 | 35.16 |
|  | HinsdaleSE | 11 | 255 | 108.64 | 45.47 |
| Green | HinsdaleNW | 38 | 255 | 115.05 | 30.44 |
|  | HinsdaleNE | 3 | 255 | 107.54 | 46.59 |
|  | HinsdaleSW | 41 | 255 | 130.16 | 35.64 |
|  | HinsdaleSE | 10 | 255 | 112.94 | 44.08 |

### 3.3 Photointerpretation

Photointerpretation of the HinsdaleNW DOQ was used for visually pre-selecting training plots to identify easily recognized examples of vegetation. Fourteen polygons representing tree canopy cover and 17 polygons representing grass or lawn were on-screen digitized (Fig. 7). Areas from various parts of the image were included to insure that each vegetation class contained a sufficient example of spectral variability.  Size of training areas ranged from 0.32 to 8.16 hectares for trees, and from 0.17 to 3.51 hectares for grass, with a total of 26.88 hectares of sample tree canopy and 12.59 hectares sample grass cover.  Due to expanses of forest preserve, it was possible to digitize fairly large polygons for tree canopy, but only smaller areas were available for lawns and grass (the larger of these being located in parks or athletic fields).  One polygon located in a carefully-maintained golf course grass was included.
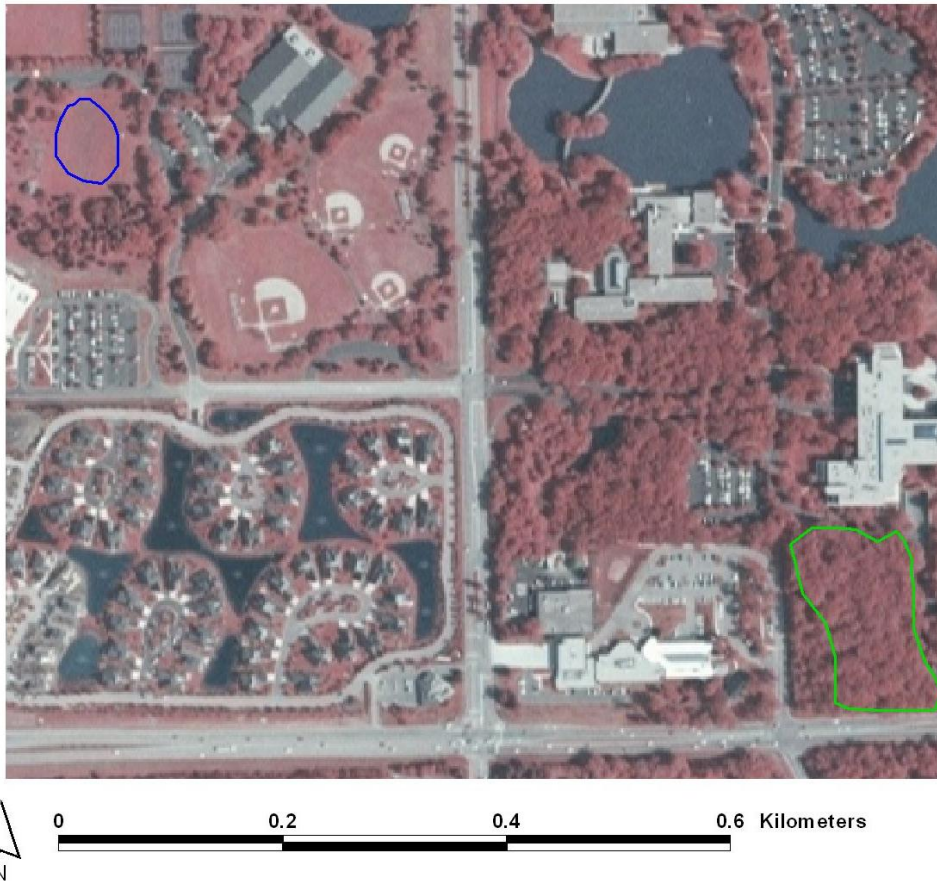
Figure 7. Portion of the HinsdaleNW color-infrared DOQ at 1:3500 detail showing examples of grass (blue) and tree canopy (green) sample polygons in a mix of impervious surface, tree canopy, and grass.

A vector dataset based on the training polygons was created for each vegetation type, then converted to raster format. The resulting rasters were used as masks when generating vegetation specific data for the individual spectral bands or vegetation indices. A third raster dataset was created by combining the tree and grass rasters into a new file where pixels representing canopy were assigned a value of one and those representing grass were assigned a value of two.

For the purposes of this study, canopy cover refers to the area, when viewed from above, that is occupied by tree crowns or shrubs. Although shrubs in the form of hedges are present in the study area, most larger hedges have been replaced by fences and the remaining extent of shrubs is not expected to have much of an effect on the canopy estimation.

### 3.4 Vegetation indices

NDVI was used to create a new raster layer incorporating pixel values from the NIR and red bands of the Hindsale NW DOQ.  In order to separate vegetation from non-vegetative pixels, a vegetation raster layer was created using only pixels with an NDVI value of greater than 0.12.  This minimum was derived from NDVI statistics returned by the grass and canopy sample plots.  Using the vegetation raster as a mask for evaluation of the tree canopy model guards against re-introduction of non-vegetation pixels in subsequent analysis.

The three individual color bands (NIR, red, and green) and nine vegetation indices were tested for ability to discriminate between urban tree canopy and grass (Table 2).  A new raster layer was created using each band or index to generate pixel values.  Using the tree canopy and grass rasters as separate masks, basic statistics were derived for each of the vegetation types.  Means, ranges, and standard deviations for tree canopy versus grass were compared for each index or spectral band.

Table 2.  Vegetation indices and equations

| Index | Band(s) used | Reference |
| --- | --- | --- |
| (spectral band) | NIR | |
| (spectral band) | Red | |
| (spectral band) | Green | |
| | | |
| NDVI | (NIR-red)/(NIR+red) | Rouse *et al*, 1973 |
| RVI or SR | NIR/red | Jordan, 1969 |
| GNDVI | (NIR-green)/(NIR+green) | Gitelson, Kaufman and Merzlyak, 1996 |
| Chlorophyll | Green/red | |
| | (Green + red + NIR)/3 | |
| | NIR/green | |
| | NIR/(green + red) | |
| | (square root of NDVI) + 0.5 | |
| | Red/(green + NIR) | |

### 3.5 Evaluation of the similarity of values between vegetation types

The means and standard deviation of grassy areas and tree canopy were compared for each index and spectral band. A t-test was considered for statistical purposes, but given the number of pixels in the samples, a significant p-value was expected for all indices tested. Instead, those indices or individual bands characterized by a large overlap of grass and canopy classes were discontinued from further evaluation. Using the mean plus or minus two standard deviations to characterize each vegetation type, a separation point midway between grass and canopy values, or their overlap, was established for each vegetation index or individual band. Classification for each index/spectral band was then completed by assigning all cells with a value above the calculated threshold to one vegetation type, and all cells containing a value equal to or below the threshold to the other vegetation type (in most cases, the vegetation with the higher values was canopy).

### 3.6 Automated classifications

Three different automated classifications of the HinsdaleNW image were also conducted for comparison with the results of the above described classification methods. Automated classifications were conducted using the three-band TIF image and the training polygons digitized for the two different vegetation types (for supervised classifications). The three automated methods were: unsupervised maximum likelihood classification; supervised maximum likelihood classification; and supervised sequential maximum a posteriori classification.

GRASS GIS maximum likelihood classification (MLC) employs a "maximum likelihood discriminant analysis classifier" (Neteler and Mitasova, 2004). In an unsupervised MLC, the maximum likelihood classifier uses cluster means and covariance matrices to determine which spectral class each cell most likely belongs in. In a supervised MLC, classification is based on spectral signatures developed from training polygons.

GRASS GIS sequential maximum a posteriori classification (SMAP) checks to see whether neighboring pixels have similar values, and aims to improve the results by assuming spatial autocorrelation. SMAP also uses a Gaussian mixture distribution to define the parameters of a spectral class given the image and training polygons. The Gaussian mixture model is particularly helpful when working with classes that contain pixels with many different spectral

17

characteristics. Tree canopy often includes many distinct spectral characteristics due to differences in species and health. The Guassian mixture distribution aims to improve segmentation performance by modeling each land cover class as a mixture of various subclasses. The clustering algorithm estimates the number of subclasses within each class, and calculates the spectral mean and covariance for each (Neteler and Mitasova, 2004).

### 3.7 Accuracy assessment

Accurate classification results are prerequisite for many environmental applications, such as urban change detection. In some cases there is a distinct pattern to the spatial distribution of classification errors that is caused by the sensor. Another common source of error in remote sensing classifications comes from assigning each pixel to a single class when many pixels are a mix of different land cover classes. Improving land cover classification accuracy has become an important theme in remote sensing literature, with several tools now commonly used to evaluate the data. A confusion matrix provides a summary of the two types of thematic error that can occur in land classification (omission, where a land cover type is underrepresented in the results, and commission, where a land cover type is overrepresented). Overall accuracy is the averaged accuracy index of each land use (in this case three: non-vegetated, tree canopy, grass) and indicates the global success of the classification. Thomlinson, Bolstad and Cohen (1999) set a target of overall accuracy of 85% with no class less than 70% accurate.

GRASS random point generator was used to create 100 testing points in HinsdaleNW. Fewer random points (75) were generated for each of the other images, as these images were used for model validation rather than model development. A simple random sampling design was considered adequate because a total of 250 points would be included after all four DOQs have been processed. Congalton (1991) maintains each land cover class in the error matrix should be represented by a minimum of 50 samples, which was accomplished by the random points evaluated across the four images (Table 3).

Table 3.  Ground truth points totals by land cover type for each image.

| HinsdaleNW | HinsdaleNE | HinsdaleSW | HinsdaleSE | Total |
|---|---|---|---|---|
| Grass 15 | Grass 25 | Grass 15 | Grass 17 | 72 |
| Canopy 39 | Canopy 27 | Canopy 24 | Canopy 28 | 118 |
| Non-vegetated 46 | Non-Vegetated 23 | Non-vegetated 36 | Non-vegetated 30 | 135 |

Using the image to ground-truth whether each point was located in grass, tree canopy, or a non-vegetated land cover, a confusion matrix was created to determine the accuracy of image classification for the HinsdaleNW DOQ.  Overall accuracy, user's accuracy, producer's accuracy and kappa coefficient were calculated.  A kappa coefficient was also calculated for the canopy class, as was the areal difference.  Following model adjustment and validation, the confusion matrix process was repeated for each of the other three images in the Hinsdale quadrangle.

**3.8 Model adjustment and validation**

In the case that none of the indices or individual bands resulted in a classification with an overall accuracy of at least 85%, the index with the highest overall accuracy would be amended using a different separation point to separate tree canopy from grass.  This revised classification would then be evaluated for accuracy.

For each index or individual band with a classification resulting in an overall accuracy of 85% or greater, a new raster dataset was created for the remaining three images in the Hinsdale quadrangle.  The test area was thereby expanded to 142.45 square kilometers in order to determine whether the best tree canopy delineation model from one DOQQ would work equally well on similar adjacent imagery.  The minimum NDVI value, as well as the vegetation type separation point for the selected index or band value, was applied to each of the other DOQQs to create three additional classifications, which were evaluated using the above accuracy assessment procedure.  A confusion matrix and related statistics were developed for each image.

Following the expansion of the study area and testing of the model on the other DOQQs, if none of the indices or spectral bands resulted in a classification with an overall accuracy of at least 85%, the index resulting in the highest overall accuracy would be examined for possible improvements based on characteristics of the specific image. For example, instead of using the separation point developed with HinsdaleNW, a formula relating that separation point to the mean or minimum values for that raster layer would be applied to each of the raster layers created for the other DOQQs. It was expected that this adjustment might be especially helpful in the case of individual bands, which will have different characteristics in each image.

When the index or spectral band that most successfully discriminated between tree canopy and grass in all four images had been identified, a raster dataset representing tree canopy in the Hinsdale quad was created by assigning all pixels meeting the tree canopy criteria established with Hinsdale NW a value of one and all other pixels a null value.

## 4. Results

### 4.1 The NDVI Layer

As expected, the NDVI layer provided a reliable means for separating vegetation from non-vegetated areas. Visual comparison of the NDVI raster with the original image reveals that roads, buildings, and water returned a negative NDVI value (Fig. 8). NDVI values for areas of tree canopy were generally higher than those for grass, but the overlap of NDVI values precluded using NDVI alone to classify the vegetation types.



Figure 8. Right: NDVI layer created from HinsdaleNW. The NDVI color table displays values less than 0.025 in white. Left: HinsdaleNW image.

Results for the raster dataset created using NDVI were used to establish a minimum NDVI value for inclusion in a vegetation layer (Table 4). Based on the mean and standard deviations of my two vegetation types, I set the minimum at 0.12 for inclusion as vegetation, treating lower values as found in grass or canopy unusual.

Table 4. General statistics for trees and grass in the NDVI raster generated for HinsdaleNW.

| | Number of pixels | Minimum pixel value | Maximum pixel value | Mean | Standard Deviation |
|---|---|---|---|---|---|
| Tree canopy | 67168 | -0.00787 | 0.30061 | 0.18549 | 0.02469 |
| Grass | 31524 | 0.07121 | 0.23913 | 0.14792 | 0.02759 |

## 4.2 Results for other vegetation indices and single bands

General statistics for eight of the additional vegetation indices [RVI, NDVI, GNDVI, NIR/green, NIR/(green+red), red/(green + NIR), (NIR+red+green)/3, square root of NDVI +0.5] indicated potential for separating the two vegetation types (Table 5). Interestingly, the chlorophyll index resulted in almost no difference in pixel values between vegetation types, and was therefore not included in further evaluations. Vegetation statistics from each individual spectral band were also different enough to indicate potential for separating tree canopy from grass (Table 6).

Table 5.  Results for pixel values in raster layers generated by additional vegetation indices. Separation point is value determined to be optimal for separating the two vegetation types. (N=67168 pixels for canopy, 31524 for grass).

| Vegetation index | Canopy Min. | Canopy Max. | Canopy mean and std dev. | Grass Min. | Grass Max. | Grass mean and std dev. | Separation Point |
|---|---|---|---|---|---|---|---|
| RVI | 0.98445 | 1.85965 | 1.45771+/-0.074155 | 1.15333 | 1.62857 | 1.34971+/-0.07771 | Grass < 1.40730 |
| GNDVI | -0.05263 | 0.25714 | 0.15791+/-0.02354 | 0.06462 | 0.20290 | 0.12403+/-0.02341 | Grass < 0.14084 |
| NIR/green | 0.90000 | 1.69231 | 1.37689+/-0.06573 | 1.13816 | 1.50909 | 1.28484+/-0.06229 | Grass < 1.32500 |
| NIR/ (green+red) | 0.47015 | 0.87603 | 0.70828+/-0.03416 | 0.57285 | 0.78182 | 0.65819+/-0.03453 | Grass < 0.68360 |
| Red/ (green+NIR) | 0.33171 | 0.48120 | 0.39751+/-0.01324 | 0.36713 | 0.46154 | 0.41727+/-0.01531 | Grass > 0.40450 |
| Chlorophyll | 0.97059 | 1.20408 | 1.05967+/-0.02107 | 0.97857 | 1.12308 | 1.05014+/-0.01728 | N/A |
| (NIR+red+green)/3 | 58 | 169 | 110.502+/-14.1326 | 105 | 170 | 141.027+/-7.02451 | Grass > 132 |
| NDVI | -0.00787 | 0.30061 | 0.18549+/-0.02469 | 0.07121 | 0.23913 | 0.14792+/-0.02759 | Grass < 0.16961 |
| Square root of NDVI +0.5 | 0.55874 | 1.04828 | 0.93014+/-0.029261 | 0.76685 | 0.98901 | 0.88297+/-0.03536 | Grass < 0.91267 |

Table 6. Results for pixel values from individual spectral bands. Separation point is value determined to be optimal for separating the two vegetation types. (N=67168 for canopy, N = 31524 for grass).

| Band | Canopy Min. | Canopy Max. | Canopy mean and std dev. | Grass Min. | Grass max. | Grass mean and std. dev. | Separation Point |
|------|-------------|-------------|--------------------------|------------|------------|--------------------------|------------------|
| NIR | 63 | 188 | 173.676+/-17.0268 | 126 | 203 | 186.099+/-7.28957 | Grass > 163 |
| Red | 46 | 159 | 94.656+/-12.9908 | 92 | 150 | 124.898+/-8.08824 | Grass > 115 |
| Green | 54 | 161 | 100.180+/-13.0861 | 99 | 161 | 131.109+/-8.00520 | Grass > 120.5 |

### 4.3 Confusion matrices and accuracy values for tested indices

Each of the spectral bands and all of the raster layers created using the eight selected vegetation indices were evaluated using 100 randomly generated ground-truth points. Overall accuracy varied from 82% for the red and green bands to 74% using NDVI (Table 7).    The kappa coefficient was highest for the red band (0.777), and while kappa for the tree canopy class was highest using the square root of NDVI + 0.5 index (0.747). The only other kappa for canopy above 0.7 was with the red/(green+NIR) index  (0.711). The lowest kappa coefficient was with NDVI (0.60), while the lowest kappa for canopy was using the unsupervised MLC (0.442). Producer's accuracy was likewise best using red band values, but the green band, (NIR+red+green)/3, and the supervised SMAP all resulted in greater than 80% producer's accuracy. The highest user's accuracy resulted from the square root of NDVI + 0.5 index (83.3), though producer's accuracy was low using this index. Red/(green+NIR) resulted in a user's accuracy greater than 80%, but the producer's accuracy was only 50%. Both the lowest user's accuracy and the lowest producer's accuracy resulted from the unsupervised MLC.

Table 7.  Accuracy assessment results for individual spectral bands and the eight indices evaluated.

| Band or Index | Overall Accuracy | Producer's accuracy for canopy | User's accuracy for canopy | Overall Kappa | Kappa for canopy |
|---|---|---|---|---|---|
| Red | 82% | 85.3 | 74.4 | 0.777 | 0.612 |
| Green | 82 | 82.4 | 73.7 | 0.703 | 0.601 |
| (NIR+red+green)/3 | 80 | 82.4 | 75.7 | 0.690 | 0.584 |
| Supvervised SMAP | 80 | 82.4 | 70.0 | 0.686 | 0.550 |
| Supervised MLC | 80 | 76.5 | 74.3 | 0.691 | 0.610 |
| NIR/green | 80 | 67.6 | 79.3 | 0.676 | 0.663 |
| Sqr root NDVI+0.5 | 79 | 58.8 | 83.3 | 0.692 | 0.747 |
| Unsuperviced MLC | 79 | 35.3 | 63.2 | 0.682 | 0.442 |
| NIR | 78 | 79.4 | 69.2 | 0.656 | 0.534 |
| GNDVI | 78 | 64.7 | 78.6 | 0.660 | 0.675 |
| NIR/(green+red) | 77 | 61.8 | 77.8 | 0.649 | 0.458 |
| Red/(green+NIR) | 76 | 50.0 | 81.0 | 0.634 | 0.711 |
| RVI | 75 | 55.9 | 73.1 | 0.616 | 0.592 |
| NDVI | 74 | 55.9 | 76.0 | 0.600 | 0.636 |

In addition to high overall accuracy, the classification by red spectral values produced the highest kappa coefficient (0.777) and held up well under visual scrutiny of the tree canopy layer overlaid on the original HinsdaleNW DOQQ (Fig. 9).  While scattered pixels in grass were included in the canopy class, where grass and trees were mixed, individual trees were often precisely mapped by the red raster layer.

Figure 9. Tree canopy raster using red spectral band values for classification (left) and original HinsdaleNW DOQQ.

The canopy raster created using green band pixel values also resulted in 82% overall accuracy, but had slightly lower producer's accuracy, user's accuracy, kappa coefficient, and kappa for canopy than the red values raster. Visual inspection revealed less grass classified as tree canopy than with the raster based on red spectral values. Both red and green band canopy rasters showed successful discrimination of individual street trees (Fig. 9 and Fig. 10).



Figure 10. Raster values classified according to green pixel value (left) and original Hinsdale NW image.

### 4.4 Application of model to other DOQQs

Based on overall accuracy as well as kappa for the canopy class, two vegetation indices (NIR/green and (NIR+red+green)/3) and two spectral bands (red and green) were selected for further evaluation with the other three Hinsdale images.

25

When the NDVI >0.12 and tree canopy threshold values were applied to these other images, the best results were with the (NIR+red+green)/3 index (Table 8). Overall accuracy ranged from 76 to 85%. Tree canopy producer's accuracy was 82.1% for HinsdaleSE, but over 95% for the other two images. Kappa ranged from 0.613 to 0.763, with kappa for canopy reaching 0.696 in HinsdaleSW.

Table 8. Accuracy assessment results for vegetation indices and spectral bands evaluated on the additional three DOQQs. Results are based on using NDVI >0.12, and grass/tree canopy cut-off for classification established during development of models with HinsdaleNW.

| Band or index | DOQQ | Overall accuracy | Producer's accuracy for canopy class | User's accuracy for canopy class | Overall Kappa | Kappa for canopy class |
|---|---|---|---|---|---|---|
| **NIR/green** | HinsdaleSW | 73% | 58.3% | 77.8% | 0.581 | 0.673 |
| | HinsdaleNE | 64 | 96.3 | 51.0 | 0.451 | 0.234 |
| | HinsdaleSE | 71 | 92.9 | 61.9 | 0.540 | 0.392 |
| **(NIR+red+ green)/3** | HinsdaleSW | 85 | 95.8 | 79.3 | 0.763 | 0.696 |
| | HinsdaleNE | 83 | 96.3 | 68.4 | 0.738 | 0.507 |
| | HinsdaleSE | 76 | 82.1 | 63.9 | 0.613 | 0.424 |
| **Green** | HinsdaleSW | 83 | 82.6 | 76.0 | 0.722 | 0.654 |
| | HinsdaleNE | 80 | 96.3 | 65.0 | 0.697 | 0.453 |
| | HinsdaleSE | 76 | 92.9 | 61.9 | 0.746 | 0.392 |
| **Red** | HinsdaleSW | 87 | 100.0 | 80.0 | 0.784 | 0.706 |
| | HinsdaleNE | 77 | 96.3 | 61.9 | 0.656 | 0.405 |
| | HinsdaleSE | 71 | 96.4 | 57.4 | 0.533 | 0.321 |

The model based on green band values, when extended to the other three images, was almost as successful as the (NIR+red+green)/3 index, with overall accuracy ranging from 71 to 83%. Producer's accuracy was consistently above 82%, though user's accuracy ranged from 61 to 76%. Overall kappa reached 0.746 with HinsdaleSE, and kappa for canopy was highest with

HinsdaleSW at 0.654.

Results using the NIR/green index were less successful with the other three DOQQs, with overall accuracy ranging from 64(NE) to 73(SW)%. Although the HinsdaleNE and HinsdaleSE had a producer's accuracy for tree canopy above 92%, user's accuracy was below 62%. Overall kappa was quite low, though kappa for the canopy class reached 0.673 with HinsdaleSW.

The model based on spectral values from the red band was likewise most successful with HinsdaleSW, was less effective with HinsdaleNE, and produced the poorest results with HinsdaleSE. Red band values resulted in the highest overall accuracy achieved in any testing during this project, however, at 87% for HinsdaleSW. HinsdaleSE only had 71% overall accuracy, while HinsdaleNE achieved 77% overall accuracy. The HinsdaleSW red band classification resulted in 100% producer's accuracy, and both HinsdaleNE and HinsdaleSE had producer's accuracy greater than 96%.

HinsdaleSE had the least successful classification using the green spectral band and the red spectral band. The only instance where this image resulted in a better classification than one of the others was using the NIR/green index, where overall accuracy was higher than with Hinsdale NE (65 vs. 71%).

For HinsdaleNW, green band values and the ratio of NIR to green were the best classifiers. For HinsdaleSW, red values and (NIR+red+green)/3 were best were most effective. For HinsdaleNE, green values and (NIR+red+green)/3 worked best. The highest overall accuracy for HinsdaleSE (76%) was produced by both the (NIR+red+green)/3 index and the green band values.

The (NIR+green+red)/3 index, or average pixel value, provided the best results for all four images combined. The overall accuracy of the final raster layer based on this index, where pixels with a value greater than 132 were classified as grass and all others as canopy, was 80.9%. This is below the limit of what can be considered a successful land classification, therefore, modification of the model was required. In order to compensate for spectral band differences between the images, the general statistics for the (NIR+green+red)/3 raster layer created for each image were examined (Table 9). Attempts to adjust the grass/canopy cut-off value to reflect differences in minimum pixel values using the formula midpoint of range * 0.86 (which was derived using the successful separation point for HinsdaleNW) slightly increased accuracy for HinsdaleNE (from 80 to 82%), but actually worsened results for HinsdaleSE.

Table 9.  Statistics for pixel values in the (NIR+red+green)/3 raster layer created for each DOQQ.

| DOQQ | Minimum | Maximum | Range | Mean | Std. Dev. | Variance |
|------|---------|---------|-------|------|-----------|----------|
| HinsdaleNW | 54 | 253 | 199 | 118.481 | 30.1768 | 910.638 |
| HinsdaleSW | 49 | 255 | 206 | 128.747 | 32.9980 | 1088.870 |
| HinsdaleNE | 32 | 254 | 222 | 114.323 | 43.0469 | 1853.040 |
| HinsdaleSE | 27 | 255 | 228 | 124.493 | 43.0934 | 1857.040 |

The green spectral band statistics for the additional three DOQQs were also examined for a connection between the best grass/tree separation point and the mean or minimum pixel value, but for HinsdaleSW and HinsdaleSE the best separation point was above the mean while for the other images the best value was below the mean.  Even by meticulous study of misclassified pixel values, it was not possible to increase HinsdaleSE's overall accuracy above 76%. Adjusting the separation point for classifying pixels as either grass or canopy to include a greater range of grass values simply resulted in more of the tree canopy being classified as grass, too. Although the HinsdaleSE green band mean was similar to the mean for HinsdaleNW, and the range in pixel values was similar to HinsdaleNE, this image did not respond as well to classification using green values.

Red spectral band values were also re-evaluated, but attempts to find a more effective separation point (much less a formula to derive it) for either HinsdaleNE or HinsdaleSE failed; experimenting with different separation values merely led to different points being misclassified.

### 4.5 Final canopy layer

Of the 325 total ground-truth points, 113 were located in canopy, 81 in grass, and 131 in non-vegetated areas (Table 10).  Of these, 100 canopy points were accurately classified, but 31 of the grass points were incorrectly classified as canopy as well.  One hundred twenty of the non-vegetation points were correctly classified, with the other 11 being misclassified as canopy. User's accuracy for the canopy class was 70.4% and producer's accuracy was 88.5%, with a mean accuracy of 78.4%.  Kappa was 0.705, with kappa for the canopy class being 0.547.  Areal difference for tree canopy was +25.7%.

Table 10.  Confusion matrix for final canopy layer.

| | | GROUND TRUTH POINTS | | | |
|---|---|---|---|---|---|
| | | Grass | Canopy | Non-vegetation | total |
| MAP DATA | Grass | 43 | 31 | 7 | 81 |
| | Canopy | 11 | 100 | 2 | 113 |
| | Non-vegetation | 0 | 11 | 120 | 131 |
| Total | | 54 | 142 | 129 | 325 |

The final canopy raster layer reveals a surprising amount of tree canopy in the suburban study area (Fig. 11).  While most actual tree canopy is included in the raster, some expanses of grass have also been classified as tree canopy.
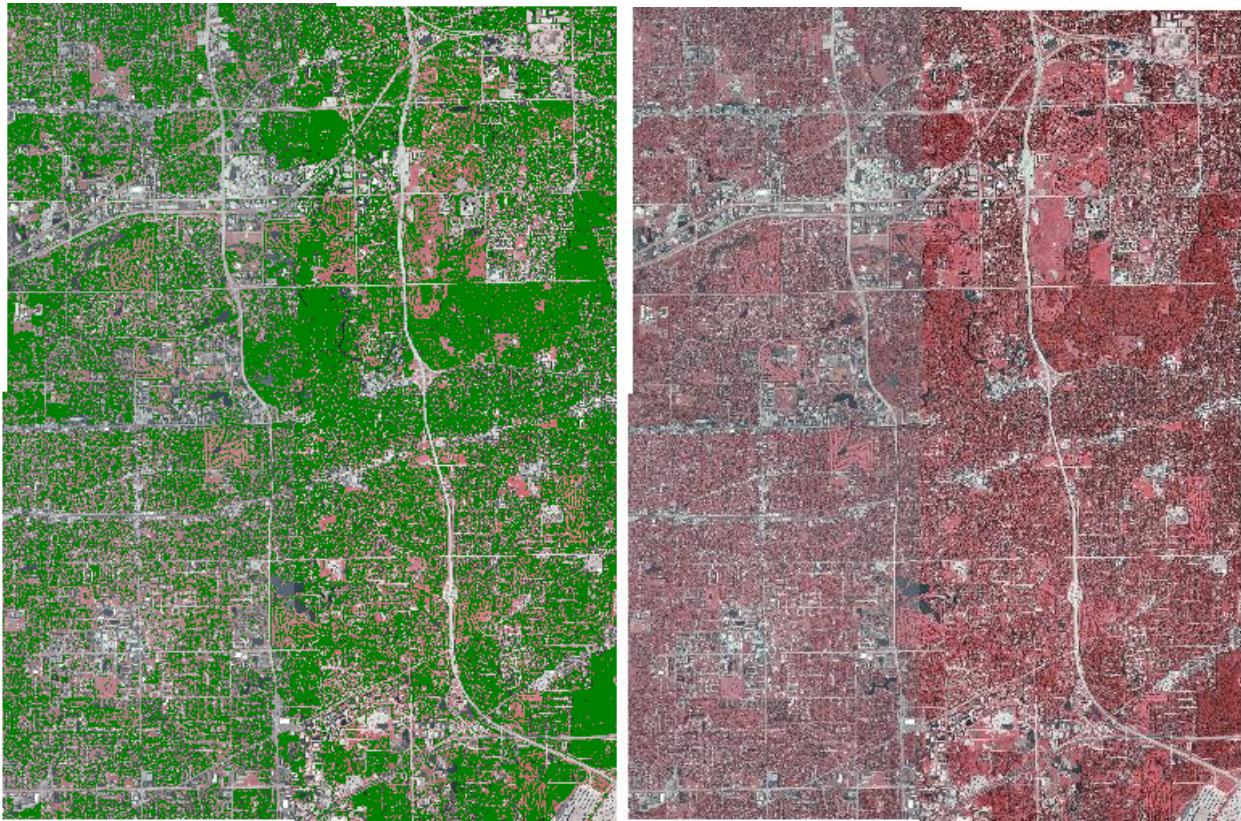


Figure 11. Final canopy layer overlaid on DOQQs (left) and original DOQQs (right).  Spectral differences are evident between the eastern and western images.

At the center of the canopy layer, where the four DOQQs converge, no glaring differences in classification results are obvious through casual visual evaluation (Fig. 12).

Figure 12. Zoom on center of Hinsdale quadrangle where four DOQQs meet: canopy cover (left), original DOQQS (right).

## 5. Discussion

### 5.1 Shadows, mixed pixels, and ground-truthing challenges

Some areas of shadow, whether on grass, tree leaves, or pavement, were classified as non-vegetated due to a low NDVI while others were included in the vegetation and classified as canopy.  Even with a two-meter resolution, mixed pixels were a problem with some ground-truth points.  Accuracy might be improved through spectral mixture analysis, but this would add to the time and complexity of the classification process, which was counter to the objective of finding a simple way to generate a canopy raster using the CIR imagery.

Other ground-truthing challenges were in the form of unusual tree species, such as the Russian olive, which has glaucous leaves and appears very pale and bright in the CIR image, hardly recognizable as a tree.  Very small patches of grass also required intense scrutiny to identify their land cover type in the images.

### 5.2 Spectral differences between DOQQs

Pixel values for all three spectral bands of HinsdaleSW were more similar to HinsdaleNW than were the eastern images, being that the western two were flown the same day.  Hence, index and spectral band values that successfully classified HinsdaleNW were more likely to be applicable to HinsdaleSW than to HinsdaleNE or HinsdaleSE.  These similarities explain why the classification of HinsdaleSW using a model developed on HinsdaleNW was more successful than applying the same model to the eastern DOQQs.  Both index models and both

individual spectral band models tested in the expanded study area produced better results with HinsdaleSW than with the eastern images.

HinsdaleNE and HinsdaleSE (flown on July 11, 2004) had lower pixel values in all three bands, especially green and red, than the western images (flown on July28, 2004) (Fig. 13). Histograms for each spectral band revealed that HinsdaleNE and HinsdaleSE pixels were skewed toward lower values. HinsdaleSE and HinsdaleNE also had higher standard deviations for each of the three spectral bands. The average humidity in Chicago on July 11, 2004 was 76, with the maximum humidity reaching 91, and light rain and scattered clouds at about 9 p.m. On July 28 the average humidity was 59, with maximum humidity reaching 90, but no rain recorded. Rather than differences in weather between the two dates, the cause of these differences might be that the images from July 11 were captured earlier in the day than the images from July 28, therefore had a brighter appearance and lower pixel values.



Figure 13. Spectral differences in DOQQS: HinsdaleNE and HinsdaleSE appear brighter than their NW and SW counterparts.

HinsdaleSE was the most difficult DOQQ to classify, with the best overall accuracy being only 76% when using the (NIR+red+green)/3 index – which was also the worst results for this index. Neither red nor green spectral values were useful for separating the two vegetation types in this image, but the NIR band, used in both indices evaluated, apparently included more useful information. Based on the poor results of classifications with this particular image, a supervised SMAP classification based on 15 polygons of each tree canopy and grass was completed, which resulted in an overall accuracy of 82%. This indicates that tree and grass values are more or less distinct in this image, just not when evaluated using the indices and spectral bands that worked best with the HinsdaleNW image.

The NIR/green index didn't work as well with the three additional images because the ratio between these bands was not the same as it was in HinsdaleNW. While NIR/green values for grass were generally lower than values for canopy in HinsdaleNW, the other images, particularly HinsdaleSE, included many NIR/green pixels where grass values that were higher than tree canopy.

Green pixel values showed good potential for separating grass from tree canopy in HinsdaleNW, but given the variability in image characteristics due to capture date and time conditions, it was unlikely that the same range of green values could be successfully applied to the other DOQQs. Green spectral band values were more variable between images than values from other bands, with differences in means ranging from 2.11 (between SE and NW) to 22.62 (between SW and NE) and, differences in minimum values ranging from 3 (between NW and SW) to 38 (between SW and NE).

Means were most similar among the DOQQs in the red band. Although these values produced the best classification using the western images, spectral differences in the eastern images rendered the threshold model ineffective.

Although red and green spectral band values produced the best tree canopy classification results using the HinsdaleNW image, it was not surprising that these results were less successful when applied to the other images. Differences in spectral band values due to variations in image capture conditions is one of the reasons vegetation indices are so widely used; the ratio between bands is relatively unaffected by these differences in imagery. Therefore, while focusing on the best method for classification tree canopy within one of these CIR images might lead to use of simple red or green spectral values, this will not be as accurate when a model developed on one

image is applied to adjacent imagery.

A more traditional image by image approach might involve harmonizing the four images by adjusting pixel value ranges in each band to a common minimum and maximum. This step was not part of this study due to the intent of developing a simple procedure that could be repeated by less proficient users. Testing against a harmonized set of images would provide another useful comparison for the effectiveness of the basic model developed.

### 5.3 Vegetation separability

Grass generally had higher values than canopy in each of the three spectral bands. In all of the indices evaluated, as well as in the red and green spectral bands, grass had more variable values than tree canopy. Though tree canopy values had greater ranges, the standard deviation of grass values was greater. This explains why user's accuracy was better than producer's accuracy for tree canopy in the models evaluated with HinsdaleNW: it was relatively simple to define the range of the majority of canopy spectral values, but not possible to filter out all of the grass values included in that range. Imagery from late August might be more effective for isolating tree canopy, as later in the summer most grass would be semi-dormant and thus have lower green and NIR values, and higher red values, while the tree canopy would be mostly unchanged (Peterson, Price and Martinko, 2002).

Heavily fertilized grass, such as golf courses or athletic fields, is usually difficult to separate from tree canopy, but the (NIR+red+green)/3 index was remarkably effective for this task (Fig. 14). This suggests that the average pixel value of grass in July CIR in this study area is notably higher than average pixel value for woody vegetation.

Figure 14. Example of golf course grass and tree canopy accurately separated (HinsdaleSW).

When producer's accuracy is much higher than user's accuracy (as in the supervised SMAP classification of HinsdaleNW), this suggests an error of commission, where tree canopy will be overrepresented due to the inclusion of pixels that actually depict other land cover types. On the other hand, results where user's accuracy is much higher than producer's accuracy (square root of NDVI +0.5, NIR/(green+red)) suggest an error of omission, where tree canopy will be underrepresented due to pixels that represent canopy being misclassified as another land cover type.

Even where confusion matrix results confirm acceptable map accuracy, visual evaluation of the resulting canopy map overlaid on the DOQQs reveal problem areas where errors of commission are obvious. Although golf courses were less of a problem than anticipated, large patches of wetland vegetation were consistently misclassified as tree canopy. Apparently the spectral values of wetland species such as cattails, sedges, and rushes are much the same as leaves on woody plants (lower than the values for grass), rendering it impossible to separate these vegetation types using CIR imagery (Fig. 15 ). Although wetland vegetation is not extensive in this suburban setting, in the locations where it does occur, the canopy map will include groups of pixels that in reality represent wetland plants. Accuracy could be improved by masking wetland areas from the dataset prior to classification.

Though canopy spectral values had relatively low variability across all indices and

spectral bands, the initial ground truth canopy plots, as well as the final ground truth points, revealed some canopy pixels with uncharacteristic spectral values. These might be caused by unhealthy or stressed trees, or perhaps species that are rare in the study area.

The grass land cover class was more poorly classified than canopy, but as a grass map was not the goal of this study, this is not a problem except in the way it impacts the canopy map. A better grass classification would mean less areal difference in the canopy class, and also an increase in user's accuracy.



Figure 15. Example of wetland vegetation (right of center and in cloverleaf) included in tree canopy class (left); original HinsdaleNW DOQQ right.

**NDVI**

The spectral value differences between the DOQQs were not surprising, but the effect this had on ratio indices was greater than expected. With a difference in image capture date of only 17 days, it is unlikely that the actual NDVI values of the vegetation changed noticeably during that time (López-Granados *et al* 2006). While the NDVI cutoff for inclusion as vegetation established with HinsdaleNW worked well with HinsdaleNE and HinsdaleSE, it caused exclusion of too much vegetation from HinsdaleSW. Closer examination of pixel values in HinsdaleSW indicated a minimum NDVI of 0.095 would have been more applicable for vegetation in this image. HinsdaleSW had the highest mean and minimum for red band values while NIR band values were more similar to the other DOQQs. Apparently the higher red band values caused a lower NDVI for vegetation in this image.

The minimum NDVI value of 0.12 is far below the 0.20 minimum NDVI for vegetation generally recognized in remote sensing literature. Kowal (2007), who used satellite imagery to

map the tree canopy of the city of Chicago, reports that NDVI values of less than 0.3 did not correspond to any tree canopy areas within his one-meter resolution merged dataset. The lower NDVI values for vegetation in the Hinsdale DOQQs is likely due to the range of wavelengths in the NIR band, which for the images in this study was 0.71 to 0.9 μm, whereas the IKONOS imagery featured in Kowal's study had a range of 0.76-0.85μm. The NIR spectral band used for NDVI generally features the shorter wavelengths from around 0.78 to 0.86 μm. Furthermore, an increase in bandwith of the NIR spectral band used can result in lower NDVI values (Teillet, Staenz and Williams,1997).

## RVI

RVI purportedly works better in dense vegetation and is not as useful in sparsely vegetated areas. Of all the indices tested, this was the only one with an overall accuracy less than that produced with the NDVI classification. With HinsdaleNW, both user's and producer's accuracy for tree canopy were below 74%. In an urban setting RVI might be effective at detecting green biomass, but not necessarily for separating the different vegetation types present.

## Chlorophyll index

This index is expected to perform better in urban areas where biomass is contrasted against a usually light background with high reflectance in both the red and NIR bands. Nichol and Lee (2005) experimented with imagery captured during the dry season in Hong Kong and found trees and grass had different spectral properties using the chlorophyll index. Apparently the dry season timing of this imagery was key to the chlorophyll index success. Spectral differences for trees and grass in the suburban Chicago imagery might have been greater in a drier year, or later in the summer. As it was, the green/red ratio did not distinguish between grass and the leaves of woody vegetation.

## (NIR+red+green)/3

Had the study begun with one of the adjacent images rather than HinsdaleNW, a different index and threshold for both NDVI and average pixel value would probably have resulted. Perhaps one of the indices that was less effective in discriminating the HinsdaleNW canopy would have been chosen for model development and extended to the other images. Without

repeating the initial evaluation and testing on each of the other three images, it is hard to be sure that there is not a template that would result in a more accurate canopy map than the one chosen through the process described in this paper, yet the average pixel value across the three CIR spectral bands does appear to retain similar values for tree canopy across these images. Further testing should apply the same NDVI and (NIR+red+green)/3 thresholds to a more distant image, or set of images. In any case, this template should only be expected to perform at the 80% accuracy level with Chicago area images acquired during the month of July; otherwise, spectral signatures could be quite different.

### 5.4 Comparison with automated classification

Although the three automated classifications were conducted only on the HinsdaleNW image, the outcome indicates that this type of classification will be less accurate than the (NIR+red+green/3) index unless time is taken to provide data for a supervised classification. Both the supervised SMAP and the supervised MLC classifications compared favorably with the (NIR+red+green)/3 index results, with the SMAP classification superior to the MLC classification only in terms of user's accuracy. If time and ability are available for the creation of supervised classification input for each image to be processed, the resulting mosaiced raster will mostly likely have an overall accuracy of at least 80%. However, the template method developed through this study is less labor intensive and produced comparable results.

### 5.5 Applicable uses for the resulting canopy layer

A raster layer created by using DOQQs, such as the four in this study, and the (NIR+red+green)/3 index can be assumed to include virtually all tree canopy. Assuming an areal difference for tree canopy of about 25%, users should adjust the total tree canopy by subtracting the amount of overrepresentation. This adjusted figure then provides a reasonable estimate of tree canopy, although further testing is required to determine how image-specific these results are. Users should also be aware of wetland vegetation occurring in their area of interest, noting that such areas will likely be misclassified as tree canopy. With this understood at the outset, they should be able to adjust their application of the data accordingly.

Because producer's accuracy is quite good, the tree canopy raster layer offers some assurance that no existing tree canopy has been omitted from the map; planners can be confident

that areas apparently lacking in tree canopy actually are. The user's accuracy is not so good, which means planners can't assume that all areas represented as canopy, especially areas known to be a grass cover, actually have trees present. For known extents of lawn, such as athletic fields, this should be relatively simple to work around. For smaller areas of grass, such as in yards around houses, it will be difficult to determine whether there is false representation of tree canopy.

### 5.6 Possible future improvements

LIDAR data has recently become freely available for some counties in the Chicago region. For those areas, application of heights returned by LIDAR might greatly improve a tree canopy map. However, LIDAR files are very large and take a long time to process. A tree canopy map generated using LIDAR would probably take a lot longer to complete.

Color balancing of the images to be mosaiced could be evaluated as a pre-classification process. Another possible avenue for improvement is a function that eliminates isolated canopy pixels in areas of grass (or grass pixels in areas of canopy), such as a 3x3 matrix filter. This would be a simple way to increase map accuracy, as isolated tree canopy pixels are almost always located in athletic fields or other lush lawn. Solving the problem of isolated misclassified pixels would also reduce the areal difference for the raster layer, but perhaps only slightly.

Also, the NAIP products may include a blue band in the future. Adding a fourth band to the CIR would likely increase the accuracy of tree canopy maps based on this imagery (Key *et al* 2001).

### 6. Conclusions

While it is possible to create a generally accurate Chicago-area tree canopy map using CIR imagery, the results will vary from image to image. In some cases, pixel values from any of the individual spectral bands will provide the best method for separating grass from the leaves of woody plants, and in other cases even vegetation indices will not be able to clearly separate the two classes. Overall accuracy greater than 85% is possible, but may fall short of 80%. Though a minimum of 0.12 NDVI for vegetation seems like a good general rule for this imagery, for some images it will be too high. If each image is evaluated and tested using training plots for the two vegetation types, as was completed for the HinsdaleNW image, accuracy will probably increase.

However, it is possible that some particular images might contain spectral characteristics that render it impossible to effectively separate grass from tree canopy.

For a quick canopy raster layer that will probably result in 80% overall accuracy, and producer's accuracy for canopy class approaching 90%, the (NIR+red+green)/3 index is the best solution when using Chicago area NAIP imagery captured during mid-summer.

## 7. References

Bowles, M. and McBride, J. 2002. Pre-European settlement vegetation of Cook County, Illinois. Report to The Cook County Forest Preserve District, Corlands & The Nature Conservancy. The Morton Arboretum, Lisle, Ill.

Buyantuyev, A., Wu, J. and Gries, C. 2007. Estimating vegetation cover in an urban environment based on Landsat ETM+ imagery: A case study in Phoenix, USA. International Journal of Remote Sensing 28(2), 20 January 2007, pp. 269-291.

Carreiras, J. M. B., Pereira, J. M.C., and Pereira, J.S. 2006. Estimation of tree canopy cover in evergreen oak woodlands using remote sensing. Forest Ecology and Management, 223, pp. 45-53.

Clevers, J. G. P. W. 1988. The derivation of a simplified reflectance model for the estimation of leaf area index, Remote Sensing of Environment, 35, pp. 53-70.

Congalton, R.G. 1991. A review of assessing the accuracy of classifications of remotely sensed data. Remote Sensing of Environment 37 pp. 35-46.

Davis, A.M. 1977. The prairie-deciduous forest ecotone in the upper middle west. Annals of the Association of American Geographers, 67 pp. 204-213.

Deering D.W., Rouse, J. W., Haas, R. H. and Schell, J.A. 1975. Measuring "forage production" of grazing units from Landsat MSS data. Proceedings of the 10th International Symposium Remote Sensing of Environment, II, pp. 1169–1178.

Gitelson, A.A., Kaufman, Y. and Merzlyak, M.N. 1996. Use of green channel in remote sensing of global vegetation from EOS-MODIS. Remote Sensing of Environment, 58, pp. 289-298.

Huete, A. R. 1988. A soil-adjusted vegetation index (SAVI). Remote Sensing of Environment, 25, pp. 295-309.

Jackson R.D. and Huege, A.R. Interpreting vegetation indices. 1991. Preventive Veterinary Medicine, 11, pp. 185-200.

Jordan, C. F. 1969. Derivation of leaf-area index from quality of light on the forest floor. Ecology, 50(4), pp. 663-666.

Key, T., Warner, T. A., McGraw, J. B. and Fajvan, M. A. 2001. A comparison of multispectral and multitemporal information in high spatial resolution imagery for classification of individual tree species in a temperate hardwood forest. Remote Sensing of Environment, 75, pp. 100-112.

Kowal, C. 2007. Measuring Urban Green. University of Illinois at Chicago College of Urban Planning and Public Affairs, student project for Masters in Urban Planning and Policy.

López-Granados, F., Jurado-Expósito, M. and Peña-Barragán, J. M. 2006. Using remote sensing for identification of late-season grass weed patches in wheat. Weed Science, 54, pp. 346-353.

Lu, D. and Weng, Q. 2004. Spectral mixture analysis of the urban landscape in Indianapolis with Landsat ETM+ imagery. Photogrammetric Engineering & Remote Sensing, 70(9), pp. 1053-1062.

Neteler, M. and Mitasova, H. 2004. Open Source GIS: a GRASS GIS Approach, 2nd ed. Springer, New York, NY, USA.

Nichol, J. and Lee, C. M. Urban vegetation monitoring in Hong Kong using high resolution multispectral images. 2005. International Journal of Remote Sensing, 26(5), pp. 903-918.

Nowak, D. J., Hoehn, R. E. III, Crane, D. E., Stevens, J. C. and Fisher, C.L. 2010. Assessing urban forest effects and values. Resource Bulletin NRS-37. Newtown Square, PA: U.S. Dept. of Agriculture, Forest Service, Northern Research Station.

Nowak, D. J., Rowntree, R. A., McPherson, E. G., Sisinni, S. M., Kerkmann, E. R. and Stevens, J.C. 1996. Measuring and analyzing urban tree cover. Landscape and Urban Planning, 36, pp. 49-57.

Peña-Barragán, J.M, Jurado-Expósito, M., López-Granados, F., Atenciano, S., Sánchez-de la Orden, M. García-Ferrer, A., and García-Torres, L. 2004. Assessing land-use in olive groves from aerial photographs. Agriculture, Ecosystems & Environment,103, pp. 117-122.

Peterson, D. L., Price, K. P. and Martinko, E. A. 2002. Discriminating between cool season and warm season grassland cover types in northeastern Kansas. International Journal of Remote Sensing, 23(23), pp. 5015-5030.

Price, K. P., Guo, X. and Stiles, J.M.  2002.  Optimal Landsat TM band combinations and vegetation indices for discrimination of six grassland types in eastern Kansas.  International Journal of Remote Sensing, 23(23), pp. 5031-5042.

Rouse, J.W., Jr., Haas, R. W., Schell, J. A., Deering, D. W. and Harlan, J.C. 1973.  Monitoring the vernal advancement and retrogradation (greenware effect) of natural vegetation. Greenbelt, MD, USA, NASA/GSFCT, Type 3, Final Report.

Teillet, P. M., Staenz, K. and Williams, D.J.  1997.  Effects of spectral, spatial, and radiometric characteristics on remote sensing vegetation indices of forested regions.  Remote Sensing of Environment, 61, pp. 139-149.

Thomlinson, J. R., Bolstad, P.V., and Cohen, W. B. 1999.  Coordinating methodologies for scaling landcover classification for ecological applications.  Remote Sensing of Environment, 72, 253-267.

Tucker, C. J.  1979.  Red and photographic infrared linear combinations for monitoring vegetation.  Remote Sensing of Environment, 8, pp. 127-150.
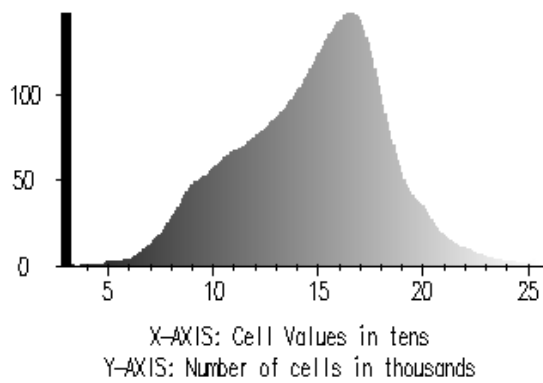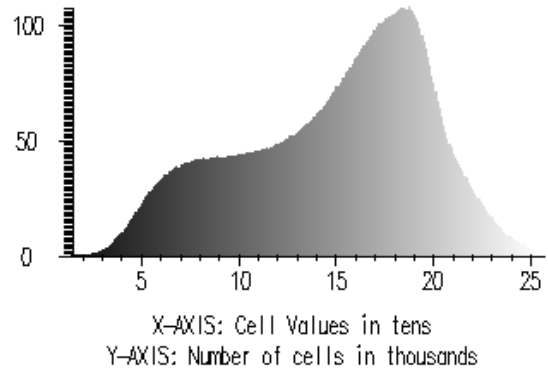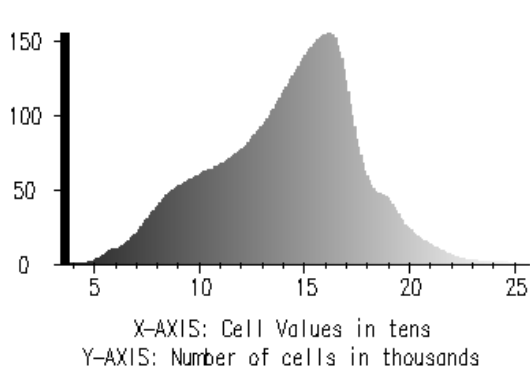
Ward, D., Phinn, S. R. and Murray, A. T.  2000.  Monitoring growth in rapidly urbanizing areas using remotely sensed data.  Professional Geographer, 53(3), pp. 371-386.

Xu, B., Gong, P.  and Pu, R.  2003.  Crown closure estimation of oak savannah in a dry season with Landsat TM imagery: comparison of various indices through correlation analysis. International Journal of Remote Sensing, 24(9), pp. 1811-1822.
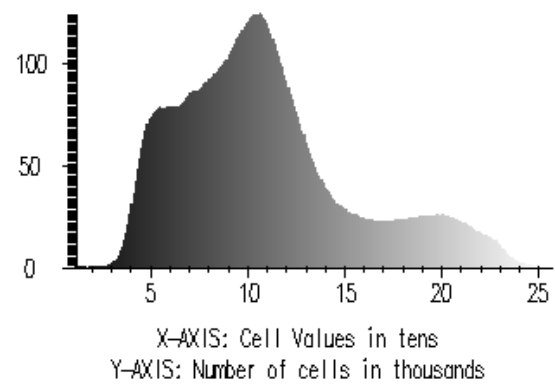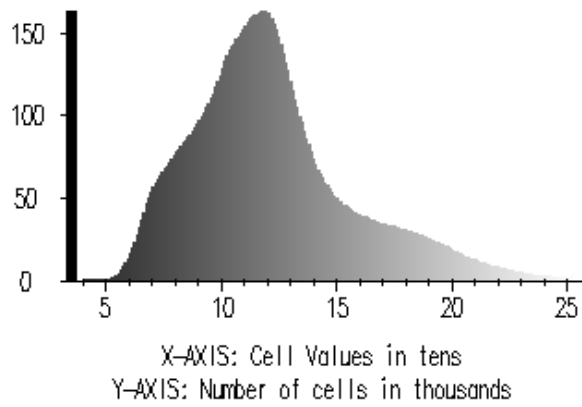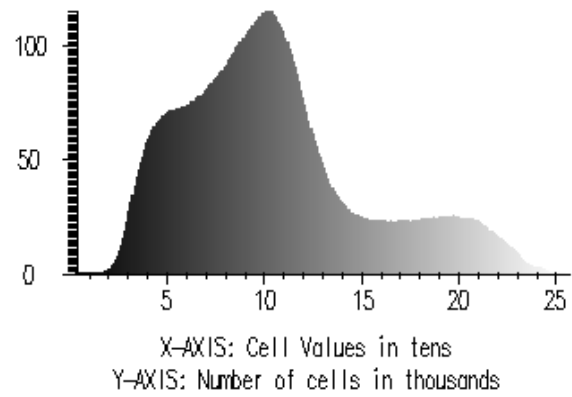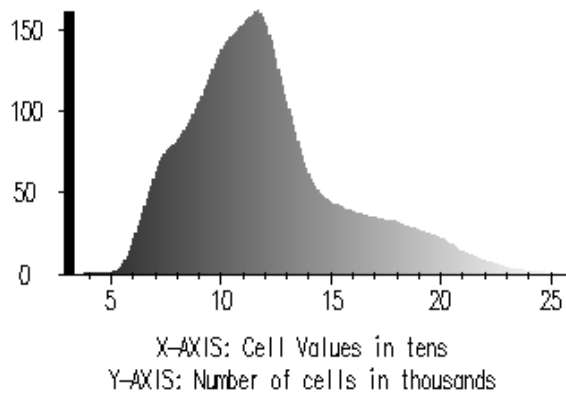
Zhou, W., Huang, G., Troy, A. and Cadenasso, M. L.  2009. Object-based land cover classification of shaded areas in high spatial resolution imagery or urban areas: a comparison study.   Remote Sensing of Environment, 113, pp. 1769-1777.
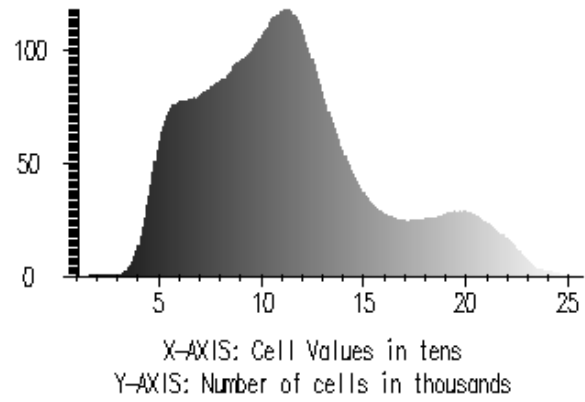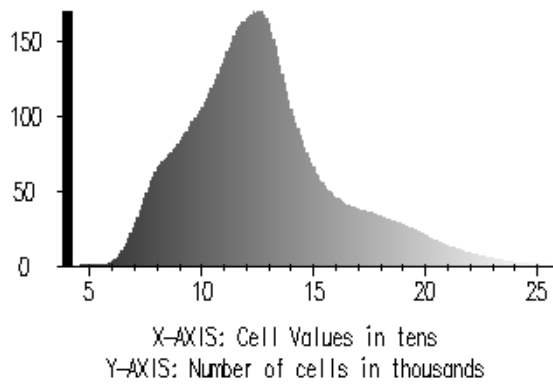
# 8. Appendices

Appendix A. Histograms for NIR band pixel values in (clockwise from upper left) HinsdaleNW, HinsdaleNE, HinsdaleSW and HinsdaleSE.



X-AXIS: Cell Values in tens
Y-AXIS: Number of cells in thousands

X-AXIS: Cell Values in tens
Y-AXIS: Number of cells in thousands

X-AXIS: Cell Values in tens
Y-AXIS: Number of cells in thousands
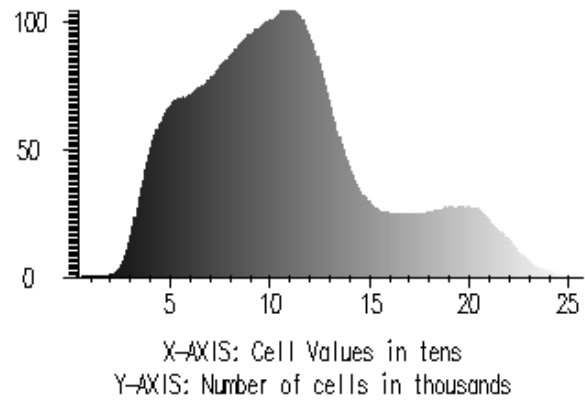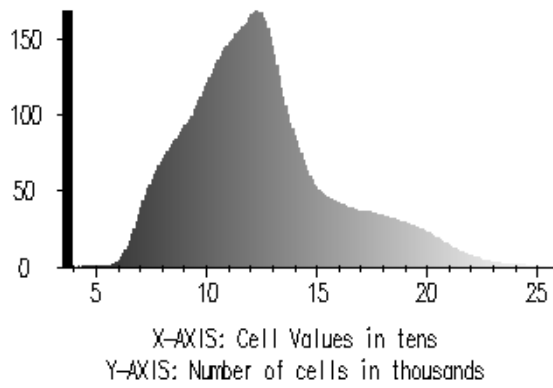
X-AXIS: Cell Values in tens
Y-AXIS: Number of cells in thousands
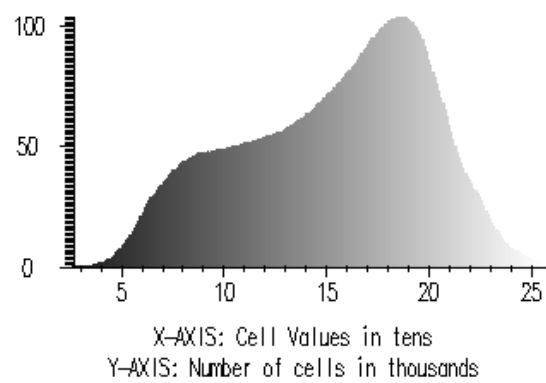
Appendix B.  Histograms for red band pixel values in (clockwise from upper left) HinsdaleNW, HinsdaleNE, HinsdaleSW and HinsdaleSE.



X–AXIS: Cell Values in tens
Y–AXIS: Number of cells in thousands



X–AXIS: Cell Values in tens
Y–AXIS: Number of cells in thousands



X–AXIS: Cell Values in tens
Y–AXIS: Number of cells in thousands



X–AXIS: Cell Values in tens
Y–AXIS: Number of cells in thousands

Appendix C.  Histograms for green band pixel values in (clockwise, from upper left)
HinsdaleNW, HinsdaleNE, HinsdaleSW and HinsdaleSE.



X–AXIS: Cell Values in tens
Y–AXIS: Number of cells in thousands

X–AXIS: Cell Values in tens
Y–AXIS: Number of cells in thousands

X–AXIS: Cell Values in tens
Y–AXIS: Number of cells in thousands

X–AXIS: Cell Values in tens
Y–AXIS: Number of cells in thousands

**Previous Reports**

Series from Lund University's Geographical Department

**Master Thesis in Geographical Information Science (LUMA-GIS)**

1. *Anthony Lawther:* The application of GIS-based binary logistic regression for slope failure susceptibility mapping in the Western Grampian Mountains, Scotland. (2008).
2. *Rickard Hansen:* Daily mobility in Grenoble Metropolitan Region, France. Applied GIS methods in time geographical research. (2008).
3. *Emil Bayramov:* Environmental monitoring of bio-restoration activities using GIS and Remote Sensing. (2009).
4. *Rafael Villarreal Pacheco:* Applications of Geographic Information Systems as an analytical and visualization tool for mass real estate valuation: a case study of Fontibon District, Bogota, Columbia. (2009).
5. *Siri Oestreich Waage:* a case study of route solving for oversized transport: The use of GIS functionalities in transport of transformers, as part of maintaining a reliable power infrastructure (2010).
6. *Edgar Pimiento:* Shallow landslide susceptibility – Modelling and validation (2010).
7. *Martina Schäfer:* Near real-time mapping of floodwater mosquito breeding sites using aerial photographs (2010)
8. *August Pieter van Waarden-Nagel:* Land use evaluation to assess the outcome of the programme of rehabilitation measures for the river Rhine in the Netherlands (2010)
9. *Samira Muhammad:* Development and implementation of air quality data mart for Ontario, Canada: A case study of air quality in Ontario using OLAP tool. (2010)
10. *Fredros Oketch Okumu*: Using remotely sensed data to explore spatial and temporal relationships between photosynthetic productivity of vegetation and malaria transmission intensities in selected parts of Africa (2011)
11. *Svajunas Plunge:* Advanced decision support methods for solving diffuse water pollution problems (2011)
12. *Jonathan Higgins:* Monitoring urban growth in greater Lagos: A case study using GIS to monitor the urban growth of Lagos 1990 - 2008 and produce future growth prospects for the city (2011).
13. *Mårten Karlberg:* Mobile Map Client API: Design and Implementation for Android (2011).
14. *Jeanette McBride:* Mapping Chicago area urban tree canopy using color infrared imagery (2012).